Acta Cryst. (1974). **B30**, 1857

The Crystal Structure of Ytterbium Metaphosphate, YbP_3O_9*

By H. Y-P. Hong

Lincoln Laboratory, Massachusetts Institute of Technology, Lexington, Massachusetts 02173, *U.S.A.*

(*Received* 14 *January* 1974; *accepted* 11 *March* 1974)

A single-crystal X-ray diffraction analysis has been performed on YbP_3O_9 synthesized by a flux method. The structure is monoclinic, with space group $P2_1/c$, $Z=12$, and cell parameters $a=11{\cdot}219$ (2), $b=19{\cdot}983$ (3), $c=9{\cdot}999$ (3) Å, $\beta=97{\cdot}30$ (2)°. A full-matrix least-squares refinement gave $R=0{\cdot}076$, $R_w=0{\cdot}064$ for 1472 independent reflections. Oxygen atoms form a tetrahedron around each P atom and an octahedron around each Yb atom. The PO_4 tetrahedra share corners to form helical ribbons running along the *c* axis. The YbO_6 octahedra are isolated from each other, with no O atom common to any two Yb atoms. The shortest Yb–Yb distance is 5·610 Å, and the concentration of Yb atoms is $5{\cdot}40\times10^{21}$ cm^{-3}. $Y_{1-x}Nd_xP_3O_9$ solid solutions appear to be promising materials for efficient Nd^{3+} lasers.

Introduction

Three types of rare-earth phosphates have been reported: orthophosphates ($LnPO_4$), metaphosphates (LnP_3O_9), and ultraphosphates (LnP_5O_{14}). The basic structure of the phosphate moiety is determined by its O/P ratio.

The O atoms in phosphates are all bonded tetrahedrally to P atoms. The PO_4 tetrahedra can be isolated from each other or share corners, but edge- and face-sharing are never observed, probably because of the repulsion between P^{5+} ions. Therefore in metaphosphates, with O/P = 3, all the tetrahedra share corners to form one-dimensional chains. As the O/P ratio increases above the critical value of 3, the chains are increasingly broken, until in orthophosphates (O/P = 4) the tetrahedra are all isolated. For O/P ratios of less than 3, as in the ultraphosphates (O/P = 2·8), the chains become cross-linked. However a three-dimensional network cannot be formed. Such a network would require each PO_4 tetrahedron to share corners with 4 others for an O/P ratio of 2, but the lower limit of this ratio is 2·5, as in P_2O_5.

In the orthophosphates the PO_4 tetrahedra are isolated from each other, while in the other compounds they share corners to form ribbons and cross-linked chains, respectively. Since the corner-sharing tetrahedra are flexible, their detailed arrangement depends on the size of the rare-earth atom, and therefore the larger rare earths (from La to Gd or Tb) form structures differently from the smaller ones (from Gd or Tb to Lu, plus Y). The orthophosphates with large Ln atoms are dimorphic-hexagonal or monoclinic (Mooney, 1948), while those with small Ln atoms are tetragonal (Schwarz, 1963). In the metaphosphate series, large Ln atoms form an orthorhombic structure (Hong, 1974), and small Ln atoms form a monoclinic structure that will be described in this paper. The ultraphosphates with large Ln atoms are monoclinic with pairs of cross-linked PO_4 chains (Hong, 1974); those with small Ln atoms have a different monoclinic structure in which all the chains in each two-dimensional layer are cross-linked (Hong & Pierce, 1974). An orthorhombic structure with pairs of cross-linked chains is formed by atoms between Dy and Er (Beucher, 1970; Durif, 1971).

We have measured a fluorescence lifetime of 490 μs for the $^4F_{3/2}$ level of Nd^{3+} in $Y_{0{\cdot}9}Nd_{0{\cdot}1}P_3O_9$, which is to be compared with 160 μs in $La_{0{\cdot}9}Nd_{0{\cdot}1}P_3O_9$ and 300 μs in $La_{0{\cdot}9}Nd_{0{\cdot}1}P_5O_{14}$ (Dwight, Hong & Pierce, 1973). In order to find an explanation for this unusually long lifetime we have used the single-crystal X-ray diffraction method to determine the structure of YbP_3O_9, which is isostructural with YP_3O_9.

Experimental procedure

Small single crystals of YbP_3O_9 were grown from a flux of 96% reagent-grade H_3PO_4 and 4% NaF by weight. A mixture of Yb_2O_3 and P_2O_5 in 1 to 5 molar ratio was combined with about half its weight of flux and preheated in a Pt crucible to 500°C for 4 h, held at 950°C for 15 h, cooled at 5°C h^{-1} to 600°C, and quenched. After being washed with hot water to dissolve any excess phosphoric acid, the product was found to include a considerable number of irregular transparent crystals with dimensions of about 0·05 to 0·2 mm.

For X-ray diffraction studies, a small crystal of about 0·1 × 0·1 × 0·1 mm was mounted on a goniometer head about the *b* axis. Oscillation and Weissenberg photographs showed diffraction symmetry $2/m$. The systematic absences were $0k0$, $k=2n+1$ and $h0l$, $l=2n+1$, which indicate uniquely the monoclinic space group $P2_1/c$ (No. 14). Values of 2θ were measured for 20 reflections carefully centered on the $K\alpha_1$ and $K\alpha_2$ components of Mo radiation ($\lambda_1=0{\cdot}70926$ Å, $\lambda_2=0{\cdot}71354$ Å), using a 1° takeoff angle and a 0·02° slit. These values were used in a least-squares refinement to deter-

---

* This work was sponsored by the Department of the Air Force.

mine the lattice parameters. Three-dimensional intensity data to $2\theta = 50°$ were collected by the stationary-crystal, stationary-counter method, using Zr-filtered Mo $K\alpha$ radiation and a 5° takeoff angle. Each peak was counted for 10 s, and the background (at 2° below the 2θ value of the peak) was counted for 10 s. In total, 3930 reflections were measured. Of these, 1472 were considered observed on the basis that the peak measurement exceeded the background by 4 counts. Only the observed reflections were used for structure analyses and refinements. Lorentz, polarization and φ-angle absorption corrections with variation less than 20% were applied. The linear absorption coefficient is 34 cm^{-1} with $\varrho_{cal} = 3{\cdot}67$ g cm^{-3}. The variance for the structure factors was calculated from

$$\sigma(F) = \tfrac{1}{2}\left[K\frac{1+I_B/I_P}{1-I_B/I_P}\right]^{1/2},$$

where I_B is the background count, I_P the peak count, and K the product of the Lorentz, polarization, and absorption corrections.

Table 1. *Final atomic parameters for* YbP_3O_9

Space group: $P2_1/c$, $Z = 12$

Cell dimensions: $a = 11{\cdot}219$ (2), $b = 19{\cdot}983$ (3), $c = 9{\cdot}999$ (3) Å, $\beta = 97{\cdot}30$ (2)°

	x	y	z	B (Å)^2
Yb(1)	0	0	0	0·44 (9)
Yb(2)	½	0	0	0·90 (9)
Yb(3)	0·0055 (3)	0·1753 (1)	0·4778 (3)	0·58 (7)
Yb(4)	0·5011 (3)	0·6570 (1)	0·0134 (3)	0·62 (8)
P(1)	0·248 (2)	0·1091 (7)	0·0256 (2)	0·3 (3)
P(2)	0·369 (2)	0·2197 (8)	0·179 (2)	0·3 (3)
P(3)	0·178 (2)	0·290 (1)	0·310 (2)	1·2 (4)
P(4)	0·226 (2)	0·447 (1)	0·978 (2)	1·6 (4)
P(5)	0·337 (2)	0·539 (1)	0·187 (2)	0·3 (3)
P(6)	0·163 (2)	0·618 (1)	0·325 (2)	1·2 (4)
P(7)	0·254 (2)	0·7751 (8)	0·012 (2)	0·5 (3)
P(8)	0·351 (2)	0·8847 (9)	0·193 (2)	0·4 (3)
P(9)	0·139 (2)	0·937 (1)	0·310 (2)	0·9 (4)
O(1)	0·234 (4)	0·998 (2)	0·358 (4)	1·0 (8)
O(2)	0·170 (4)	0·060 (2)	0·067 (4)	2·5 (9)
O(3)	0·375 (4)	0·087 (2)	0·006 (4)	1·1 (8)
O(4)	0·127 (4)	0·091 (2)	0·450 (4)	0·8 (7)
O(5)	0·353 (4)	0·088 (2)	0·453 (4)	0·7 (7)
O(6)	0·253 (4)	0·170 (3)	0·126 (4)	2·5 (9)
O(7)	0·454 (4)	0·176 (3)	0·263 (4)	2·4 (9)
O(8)	0·115 (4)	0·249 (2)	0·407 (4)	1·5 (8)
O(9)	0·384 (5)	0·271 (2)	0·080 (5)	3·6 (9)
O(10)	0·277 (5)	0·271 (2)	0·245 (5)	2·9 (9)
O(11)	0·093 (5)	0·302 (2)	0·183 (5)	2·9 (9)
O(12)	0·199 (4)	0·357 (2)	0·375 (3)	1·1 (6)
O(13)	0·242 (4)	0·479 (2)	0·118 (4)	1·0 (8)
O(14)	0·404 (4)	0·518 (2)	0·307 (4)	0·9 (8)
O(15)	0·355 (4)	0·592 (2)	0·094 (4)	1·3 (8)
O(16)	0·099 (3)	0·586 (2)	0·432 (3)	0·6 (6)
O(17)	0·216 (4)	0·591 (2)	0·210 (4)	2·2 (8)
O(18)	0·055 (4)	0·657 (2)	0·223 (4)	0·9 (8)
O(19)	0·248 (4)	0·667 (2)	0·392 (5)	0·9 (8)
O(20)	0·137 (5)	0·756 (3)	0·031 (5)	2·9 (9)
O(21)	0·354 (6)	0·819 (3)	0·119 (6)	4·0 (9)
O(22)	0·345 (4)	0·780 (2)	0·473 (4)	1·3 (7)
O(23)	0·439 (4)	0·874 (2)	0·315 (4)	2·0 (9)
O(24)	0·102 (3)	0·905 (2)	0·428 (3)	0·6 (6)
O(25)	0·209 (4)	0·893 (2)	0·225 (4)	1·7 (8)
O(26)	0·362 (4)	0·941 (2)	0·099 (4)	2·1 (9)
O(27)	0·048 (4)	0·964 (2)	0·212 (4)	0·7 (6)

Table 2. *Bond distances* (Å) *and angles* (°) *for* YbP_3O_9

Octahedron around Yb(1)

Yb(1)–O(2)	2 × 2·28 (4)	O(2)—Yb(1)–O(16)	86 (1)
Yb(1)–O(16)	2 × 2·20 (4)	O(2)—Yb(1)–O(16)	94 (1)
Yb(1)–O(27)	2 × 2·23 (4)	O(2)—Yb(1)–O(27)	102 (1)
O(2)—Yb(1)–O(2)	180	O(2)—Yb(1)–O(27)	78 (1)
O(16)–Yb(1)–O(16)	180	O(16)–Yb(1)–O(27)	92 (1)
O(27)–Yb(1)–O(27)	180	O(16)–Yb(1)–O(27)	88 (1)

Octahedron around Yb(2)

Yb(2)–O(3)	2 × 2·24 (4)	O(3)—Yb(2)–O(14)	95 (1)
Yb(2)–O(14)	2 × 2·12 (4)	O(3)—Yb(2)–O(14)	85 (1)
Yb(2)–O(26)	2 × 2·27 (4)	O(3)—Yb(2)–O(26)	86 (1)
O(3)—Yb(2)–O(3)	180	O(3)—Yb(2)–O(26)	94 (1)
O(14)–Yb(2)–O(14)	180	O(14)–Yb(2)–O(26)	89 (1)
O(26)–Yb(2)–O(26)	180	O(14)–Yb(2)–O(26)	91 (1)

Octahedron around Yb(3)

Yb(3)–O(4)	2·21 (4)	O(4)—Yb(3)–O(8)	95 (2)
Yb(3)–O(8)	2·10 (4)	O(4)—Yb(3)–O(11)	94 (2)
Yb(3)–O(11)	2·21 (5)	O(4)—Yb(3)–O(18)	83 (2)
Yb(3)–O(18)	2·07 (4)	O(4)—Yb(3)–O(24)	83 (1)
Yb(3)–O(20)	2·26 (6)	O(8)—Yb(3)–O(11)	88 (2)
Yb(3)–O(24)	2·28 (4)	O(8)—Yb(3)–O(18)	86 (2)
O(4)—Yb(3)–O(20)	169 (2)	O(8)—Yb(3)–O(20)	86 (2)
O(8)—Yb(3)–O(18)	175 (2)	O(11)–Yb(3)–O(20)	97 (2)
O(11)–Yb(3)–O(18)	172 (2)	O(11)–Yb(3)–O(24)	88 (1)
		O(18)–Yb(3)–O(20)	87 (2)
		O(18)–Yb(3)–O(24)	99 (1)
		O(20)–Yb(3)–O(24)	96 (2)

Octahedron around Yb(4)

Yb(4)–O(5)	2·13 (4)	O(5)—Yb(4)–O(7)	83 (2)
Yb(4)–O(7)	2·26 (4)	O(5)—Yb(4)–O(9)	91 (2)
Yb(4)–O(9)	2·22 (5)	O(5)—Yb(4)–O(15)	98 (2)
Yb(4)–O(15)	2·31 (4)	O(5)—Yb(4)–O(23)	97 (2)
Yb(4)–O(22)	2·15 (4)	O(7)—Yb(4)–O(9)	104 (2)
Yb(4)–O(23)	2·11 (4)	O(7)—Yb(4)–O(15)	80 (2)
O(5)—Yb(4)–O(22)	175 (2)	O(7)—Yb(4)–O(22)	99 (2)
O(7)—Yb(4)–O(23)	170 (2)	O(9)—Yb(4)–O(22)	93 (2)
O(9)—Yb(4)–O(15)	171 (2)	O(9)—Yb(4)–O(23)	86 (2)
		O(15)–Yb(4)–O(22)	78 (2)
		O(15)–Yb(4)–O(23)	90 (2)
		O(22)–Yb(4)–O(23)	80 (2)

Tetrahedron around P(1)

				Angles of O–P–O
P(1)–O(2)	1·41 (4)	O(2)–O(3)	2·51 (6)	117 (3)
P(1)–O(3)	1·53 (5)	O(2)–O(6)	2·44 (6)	109 (3)
P(1)–O(6)	1·57 (5)	O(2)–O(12)	2·58 (6)	113 (3)
P(1)–O(12)	1·68 (3)	O(3)–O(6)	2·52 (6)	110 (3)
		O(3)–O(12)	2·47 (6)	102 (2)
		O(6)–O(12)	2·56 (6)	104 (2)

Tetrahedron around P(2)

P(2)–O(6)	1·67 (5)	O(6)–O(7)	2·47 (6)	104 (3)
P(2)–O(7)	1·47 (5)	O(6)–O(9)	2·55 (6)	111 (3)
P(2)–O(9)	1·45 (5)	O(6)–O(10)	2·34 (6)	90 (3)
P(2)–O(10)	1·65 (5)	O(7)–O(9)	2·68 (6)	133 (3)
		O(7)–O(10)	2·72 (6)	122 (3)
		O(9)–O(10)	2·16 (6)	88 (3)

Tetrahedron around P(3)

P(3)–O(8)	1·51 (4)	O(8)—O(10)	2·62 (6)	128 (3)
P(3)–O(10)	1·41 (6)	O(8)—O(11)	2·48 (6)	109 (3)
P(3)–O(11)	1·51 (6)	O(8)—O(12)	2·40 (6)	106 (2)
P(3)–O(12)	1·49 (4)	O(10)–O(11)	2·18 (6)	96 (3)
		O(10)–O(12)	2·38 (6)	111 (3)
		O(11)–O(12)	2·41 (6)	106 (2)

Table 2 (*cont.*)

Tetrahedron around P(4)

P(4)–O(1)	1·64 (4)	O(1)–O(4)	2·46 (6)	110 (3)
P(4)–O(4)	1·35 (5)	O(1)–O(5)	2·36 (6)	92 (2)
P(4)–O(5)	1·63 (5)	O(1)–O(13)	2·63 (6)	112 (2)
P(4)–O(13)	1·53 (4)	O(4)–O(5)	2·53 (6)	116 (3)
		O(4)–O(13)	2·42 (6)	115 (3)
		O(5)–O(13)	2·56 (6)	108 (3)

Tetrahedron around P(5)

P(5)–O(13)	1·69 (5)	O(13)–O(14)	2·57 (6)	112 (3)
P(5)–O(14)	1·40 (5)	O(13)–O(15)	2·61 (6)	113 (2)
P(5)–O(15)	1·44 (4)	O(13)–O(17)	2·47 (6)	91 (2)
P(5)–O(17)	1·75 (5)	O(14)–O(15)	2·59 (6)	132 (3)
		O(14)–O(17)	2·65 (6)	114 (3)
		O(15)–O(17)	2·06 (6)	80 (2)

Tetrahedron around P(6)

				Angles of O–P–O
P(6)–O(16)	1·50 (4)	O(16)–O(17)	2·72 (6)	133 (3)
P(6)–O(17)	1·46 (4)	O(16)–O(18)	2·53 (6)	105 (2)
P(6)–O(18)	1·67 (5)	O(16)–O(19)	2·39 (6)	107 (3)
P(6)–O(19)	1·47 (5)	O(17)–O(18)	2·25 (6)	91 (2)
		O(17)–O(19)	2·35 (6)	107 (3)
		O(18)–O(19)	2·60 (6)	110 (3)

Tetrahedron around P(7)

P(7)–O(19)	1·66 (5)	O(19)–O(20)	2·52 (6)	110 (3)
P(7)–O(20)	1·40 (6)	O(19)–O(21)	2·45 (6)	93 (3)
P(7)–O(21)	1·69 (6)	O(19)–O(22)	2·60 (6)	106 (2)
P(7)–O(22)	1·58 (5)	O(20)–O(21)	2·82 (6)	128 (3)
		O(20)–O(22)	2·59 (6)	119 (3)
		O(21)–O(22)	2·47 (6)	97 (3)

Tetrahedron around P(8)

P(8)–O(21)	1·51 (6)	O(21)–O(23)	2·30 (6)	103 (3)
P(8)–O(23)	1·48 (5)	O(21)–O(25)	2·53 (6)	105 (3)
P(8)–O(25)	1·67 (5)	O(21)–O(26)	2·44 (6)	110 (3)
P(8)–O(26)	1·48 (4)	O(23)–O(25)	2·63 (6)	114 (3)
		O(23)–O(26)	2·60 (6)	122 (3)
		O(25)–O(26)	2·45 (6)	102 (2)

Tetrahedron around P(9)

P(9)–O(1)	1·65 (5)	O(1)—O(24)	2·54 (6)	109 (2)
P(9)–O(24)	1·45 (4)	O(1)—O(25)	2·48 (6)	103 (3)
P(9)–O(25)	1·51 (5)	O(1)—O(27)	2·50 (6)	107 (3)
P(9)–O(27)	1·43 (5)	O(24)–O(25)	2·51 (6)	115 (3)
		O(24)–O(27)	2·47 (6)	118 (3)
		O(25)–O(27)	2·30 (6)	102 (3)

Inter-tetrahedral angles

P(4)–O(1)—P(9)	128 (3)	P(5)–O(17)–P(6)	136 (3)
P(1)–O(6)—P(2)	129 (3)	P(6)–O(19)–P(7)	139 (3)
P(2)–O(10)–P(3)	157 (4)	P(7)–O(21)–P(8)	135 (5)
P(1)–O(12)–P(3)	140 (3)	P(8)–O(25)–P(9)	138 (3)
P(4)–O(13)–P(5)	132 (3)		

Structure determination

The heavy-atom method was used to solve the structure. It was observed that the reflections with $k=3n$ were stronger than the others. This indicates that heavy atoms have a repeat distance of one-third of the b axis. A three-dimensional Patterson map showed distinct strong interactions at $(\frac{1}{2},0,0)$, $(0,\frac{1}{6},\frac{1}{2})$, $(\frac{1}{2},\frac{1}{6},\frac{1}{2})$, $(0,\frac{1}{3},0)$, $(\frac{1}{2},\frac{1}{3},0)$, $(0,\frac{1}{2},\frac{1}{2})$, and $(\frac{1}{2},\frac{1}{2},\frac{1}{2})$, from which it was concluded that 12 Yb atoms are located in four independent positions, at 2(*a*), 2(*b*) and two sets of 4(*e*) in space group $P2_1/c$. A structure-factor calculation based on these positions gave a value of 0·280 for the difference function $R=\sum|F_o-F_c|/\sum|F_o|$. Published scattering factors for Yb^{3+}, P and O (Cromer

Table 3. *Structure factors*

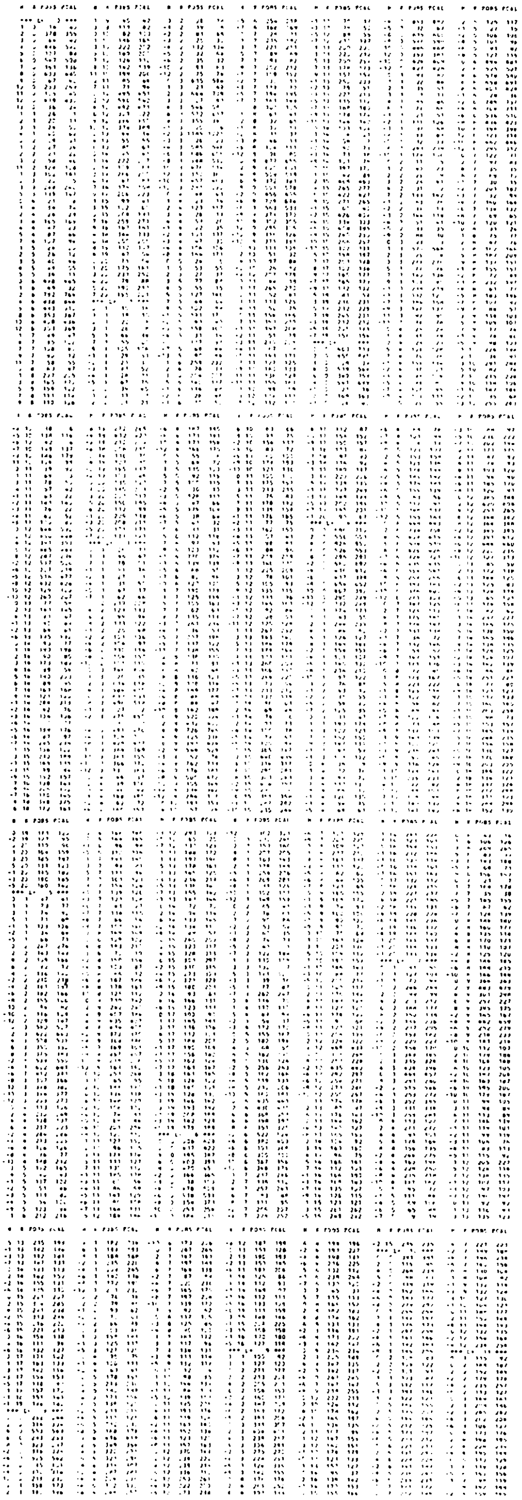

& Waber, 1965) and anomalous dispersion coefficients for Mo radiation (Cromer, 1965) were used in this and subsequent calculations. A difference Fourier map based on this model did not give a reasonable P atom arrangement. Alternative models were constructed, all taking account of the fact that in metaphosphates (O/P = 3) the PO_4 tetrahedra share corners to form one-dimensional chains. For the best of these models, with nine independent P atoms, R was reduced to 0·178. A subsequent difference Fourier map clearly revealed 27 independent O positions. The atomic parameters and isotropic temperature factors were then refined, using a full-matrix least-squares program (Prewitt, 1962). Their final values are listed in Table 1, and the bond distances and angles are listed in Table 2. Table 3 gives the observed and calculated structure factors. For all observed reflections, $R=0{\cdot}076$ and the weighted $R_w=0{\cdot}064$, where $R_w=[\sum w(F_o-F_c)^2/\sum wF_o^2]^{1/2}$ with $w=1/\sigma^2$. In the final cycle the maximum and average shift/error are 0·61 and 0·11, respectively. No correction was made for secondary extinction. A final difference synthesis revealed no physically significant peaks.

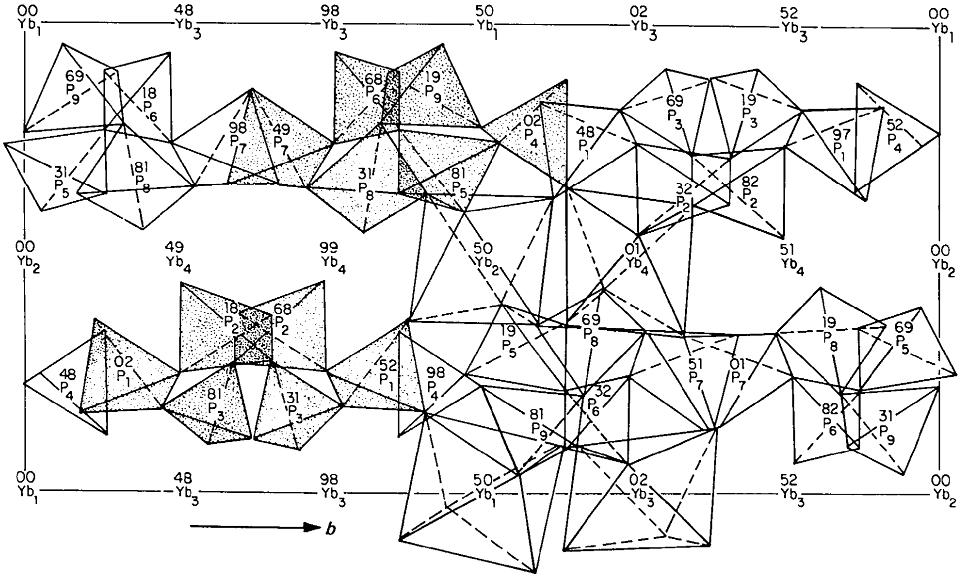

Fig. 1. An *ab* projection of the arrangement of PO_4 tetrahedra and YbO_6 octahedra in YbP_3O_9. The octahedra are slightly distorted.

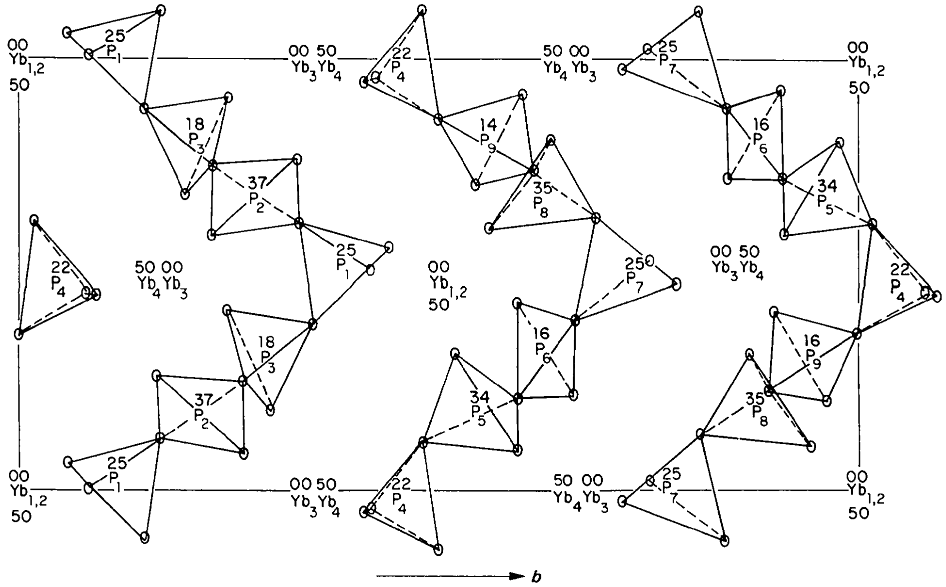

Fig. 2. A *bc* projection of the arrangement of PO_4 tetrahedra in YbP_3O_9, showing the ribbons that run helically along the *c* axis.

Discussion

The structure of YbP_3O_9 is illustrated in Figs. 1 and 2. The basic structural units are helical ribbons, $(PO_3)_n$, formed by corner-sharing of PO_4 tetrahedra. The ribbons run along the *c* axis and are joined to each other by Yb–O bonds. Each Yb atom is coordinated with six O atoms to form slightly distorted octahedra that are isolated from each other. The shortest Yb–Yb distance is 5·610 Å. Each O atom is bonded to two cations, either two P atoms or one P and one Yb atom; no O atom is common to two Yb atoms. In contrast, in NdP_3O_9 every Nd atom shares two O atoms with a second Nd atom. In that structure, each Nd atom is coordinated to eight O atoms. Most P–O distances are longer for O atoms bonded to two P atoms than for those bonded to one P and one Yb atom, probably because of the repulsion between P^{5+} ions. Longer bond distances in P–O–P bonding were also observed in NdP_3O_9, NdP_5O_{14} (Hong, 1974) and YbP_5O_{14} (Hong & Pierce, 1974). Due to ionic repulsion, P^{5+} ions do not form edge-shared tetrahedra, although they can exhibit corner-sharing. Because of their increased charge, Mo^{6+}, W^{6+} or Re^{7+} can form only isolated tetrahedra.

The fact that the Nd^{3+} fluorescence lifetime is considerably longer in $Y_{0.9}Nd_{0.1}P_3O_9$ (490 μs) than in $La_{0.9}Nd_{0.1}P_3O_9$ (160 μs) can be attributed in part to the reduction in Nd–Nd pair interactions and therefore to reduction of concentration quenching in the YbP_3O_9 structure because of the isolation of the rare-earth ions from each other. The difference also results in part because the limiting lifetime for very dilute solutions of Nd^{3+} in YP_3O_9 is at least 490 μs, compared with 375 and 325 μs for such solutions in LaP_3O_9 and LaP_5O_{14}, respectively (Dwight, Hong & Pierce, 1973).

The observation of a particularly high lifetime in $Y_{0.9}Nd_{0.1}P_3O_9$ makes the $Y_{1-x}Nd_xP_3O_9$ solid solution a source of promising materials for efficient Nd^{3+} lasers. Another potential advantage is that the concentration of rare-earth ions in the YbP_3O_9 structure is $5{\cdot}4\times10^{21}$ cm^{-3}, compared with only $3{\cdot}9\times10^{21}$ cm^{-3} in $La_{1-x}Nd_xP_5O_{14}$ solid solutions, which have already been used for the fabrication of lasers. However, since YP_3O_9 and NdP_3O_9 have different structures, the solubility of Nd^{+3} in YP_3O_9 must be limited. The maximum value of the solubility was observed about $x=0{\cdot}20$ in the series of $Y_{1-x}Nd_xP_3O_9$.

The author is grateful to Dr A. J. Strauss for helpful discussions, to K. Dwight Jr for fluorescence lifetime measurements, and to C. H. Anderson Jr for chemical preparations, X-ray data collection, and technical assistance.

References

Beucher, M. (1970). *Les Elements des Terres Rares*, Coll. No. 180, Vol. 1, pp. 331–336. Paris: CNRS.
Cromer, D. T. (1965). *Acta Cryst.* **18**, 17–23.
Cromer, D. T. & Waber, J. T. (1965). *Acta Cryst.* **18**, 107–109.
Durif, A. (1971). *Bull. Soc. Fr. Minér. Crist.* **94**, 314–318.
Dwight, K. Jr, Hong, H. Y-P. & Pierce, J. W. (1973). *Solid State Research Report, Lincoln Laboratory, M.I.T.* (1973:3), 47–48, DDC AD-770 293/9.
Hong, H. Y-P. (1974). *Acta Cryst.* B**30**, 468–474.
Hong, H. Y-P. & Pierce, J. W. (1974). *Mat. Res. Bull.* In the press.
Mooney, R. C. L. (1948). *J. Chem. Phys.* **16**, 1003.
Prewitt, C. T. (1962). *SFLS* 23, Least Squares Refinement Program, M.I.T., Cambridge, Mass.
Schwarz, H. (1963). *Z. anorg. allgem. Chem.* **323**, 44.

Acta Cryst. (1974). B**30**, 1861

The Crystal Structure of t-Amyloxycarbonyl-L-prolyl-L-prolyl-L-proline

By G. Kartha,[*] T. Ashida and M. Kakudo

Institute for Protein Research, Osaka University, Suita 565, *Japan*

(*Received* 4 *February* 1974; *accepted* 18 *March* 1974)

The crystal is orthorhombic, space group $P2_12_12_1$, with $a=14{\cdot}315$, $b=9{\cdot}924$, $c=15{\cdot}916$ Å, $Z=4$. 1897 non-zero reflexions collected on a diffractometer ($\sin\theta/\lambda=0{\cdot}575$) were used in the structure determination. The structure was solved by the symbolic addition method and refined by the least-squares method to an R of 0·06. The steric hindrance between pyrrolidine rings of nearest neighbours significantly affects the bond angles of the peptide linkages in order to suppress the effect of overcrowding. One of the C^{γ} atoms of a pyrrolidine ring shows remarkable anomalous behaviour. The peptide bonds are *trans*, and the conformation of the peptide chains is fairly close to those of poly-L-proline II.

Introduction

X-ray studies on a group of synthetic peptides, which are related to collagen as collagenase substrates or as collagen model polypeptides, have been carried out as one of the main research projects in this laboratory. The present study of the crystal structure of t-amyloxycarbonyl-L-prolyl-L-prolyl-L-proline is part of this project. Conformational studies of proline oligomers carried out recently by spectroscopic methods revealed the following structural characteristics (Isemura,

---

[*] On leave from Roswell Park Memorial Institute, Buffalo, N.Y. 14203, U.S.A.